

## Non-gray Radiation with Turbulent Convection in the Entrance Region of a Smooth Tube

매끈한 튜브의 입구 영역에서 난류유동에 의한 대류와 비회복사

서 태 범\*  
T. B. Seo

**Key words :** Non-gray radiation(비회복사), P-1 approximation(P-1 근사법), Turbulent flow(난류 유동), Radiative Nusselt number(복사뉴셀트수), Entrance region(입구영역), Exponential wide band model(지수광폭밴드모형)

### 요 지

튜브 내의 입구영역에서 난류 유동에 의한 대류와 비회복사(non-gray radiation)가 동시에 일어날 때의 열전달특성을 수치해석적으로 연구하였다. 작동유체는 이산화탄소, 수증기, 질소의 혼합가스라고 가정하였다. 지배방정식을 계산하기 위해 유한차분법이 이용되었고, 복사전달방정식을 이차편미분방정식으로 바꾸기 위해 P-1 근사법이 사용되었다. 그리고 혼합가스의 비회흡수계수(non-gray absorption coefficient)는 지수광폭밴드모형(exponential wide band model)을 이용해서 구하였다. 열전달특성에 대한 온도조건의 영향을 조사하기 위해 튜브의 축방향에 대한 평균 온도와 뉴셀트수(Nusselt number)의 변화를 몇 가지 다른 온도조건에 대해 나타내었다. 또한, 가스의 성분조성에 대한 영향을 조사하였으며, 이러한 결과에 기초해서 튜브 내에서 난류유동에 의한 대류와 비회복사가 동시에 일어날 때의 복사 뉴셀트수를 쉽게 예측할 수 있는 방법을 제시하였다.

### NOMENCLATURE

<p><math>A</math> : area, <math>m^2</math></p> <p><math>a</math> : absorption coefficient, <math>m^{-1}</math></p> <p><math>c_1, c_2, c_\mu</math> : turbulence model constants</p> <p><math>c_p</math> : specific heat at constant pressure, <math>J/kgK</math></p> <p><math>D</math> : diameter, <math>m</math></p> <p><math>dp/dx</math> : axial pressure gradient, <math>Pa/m</math></p> <p><math>e_b</math> : black body emissive power, <math>W/m^2</math></p> <p><math>F_c</math> : the correction factor(the ratio of <math>q_{cal}</math> to <math>q_{mbl}</math>. see Eq.(24))</p>	<p><math>G</math> : integrated radiation intensity, <math>W/m^2</math></p> <p><math>h</math> : heat transfer coefficient, <math>W/m^2K</math></p> <p><math>k</math> : thermal conductivity, <math>W/mK</math>, or turbulent kinetic energy, <math>m^2/s^2</math></p> <p><math>Le</math> : mean beam length, <math>m(=3.6 V/A</math>, see Siegel and Howell(10))</p> <p><math>Nu</math> : Nusselt number</p> <p><math>P</math> : pressure, <math>Pa</math>, or production of turbulent kinetic energy, <math>m^2/s^3</math></p> <p><math>Pr</math> : Prandtl number</p> <p><math>Pr_t</math> : turbulent Prandtl number</p> <p><math>q</math> : heat flux, <math>W/m^2</math></p> <p><math>q_{cal}</math> : the axial local heat flux calculated by</p>
--	--

\* 삼성코닝 생산기술과 기술일류화팀

	the present numerical model, W/m <sup>2</sup>
$q_{mN}$	: the radiation heat flux evaluated by the mean beam length model, W/m <sup>2</sup>
$\bar{q}_r$	: radiative heat flux vector, W/m <sup>2</sup>
$R$	: radius, m
$r, x$	: cylindrical coordinates
$Re$	: Reynolds number $\left( = \frac{VD}{\nu} \right)$
$T$	: temperature, K
$T_g$	: gas temperature, K
$T_m$	: bulk mean temperature $\left( = \frac{\int_0^R u T r dr}{\int_0^R u r dr} \right) K$
$T_b$	: bulk temperature $(= (T_{in} + T_{out})/2)$ , K
$t^*$	: nondimensional near-wall temperature $\left( = \frac{(T_w - T) \sqrt{\tau_w / \rho}}{q_w / (\rho c_p)} \right)$
$u, v$	: velocity components in cylindrical coordinate, m/s
$u_\tau$	: friction velocity $(= \sqrt{\tau_w / \rho})$ , m/s
$u^*$	: nondimensional near-wall velocity $(= u/u_\tau)$
$V$	: mean velocity, m/s, or volume, m <sup>3</sup>
$x^*$	: dimensionless length $\left( = \frac{x}{D_h \cdot Re \cdot Pr} \right)$
$Y$	: mole fraction
$y^*$	: nondimensional near-wall displacement $\left( = \frac{y u_\tau}{\nu} \right)$
$\varepsilon$	: dissipation of turbulent kinetic energy, m <sup>2</sup> /s <sup>3</sup>
$\nu$ or $\nu_e$	: Kinematic viscosity, m <sup>2</sup> /s
$\nu_t$	: eddy viscosity, m <sup>2</sup> /s
$\rho$	: density, kg/m <sup>3</sup>
$\sigma_k, \sigma_\varepsilon$	: empirical constant for turbulence model
$\tau$	: shear stress

### Subscripts

c : convective

$i$	: $i^{\text{th}}$ band
in	: inlet
l	: laminar
m	: mean
out	: outlet
r	: radiative
t	: total
w	: wall

## 1. INTRODUCTION

Different types of high temperature heat exchangers (above 500°C) are widely used in industry. For example, fire-tube boilers are used to supply steam, and recuperators and regenerators are used to recover waste heat from high temperature exhaust gases. In order to optimally design a high temperature heat exchanger and to evaluate its performance, a thorough analysis of the heat transfer characteristics in a heat exchanger element is required. The working fluids in these applications are usually products of combustion consisting mainly of carbon dioxide, water vapor, and nitrogen. Carbon dioxide and water vapor can emit and absorb thermal radiation, and the absorptivity is a strong function of wave number and temperature. Therefore, not only convective heat transfer but also non-gray radiative heat transfer in the participating media must be considered in any analysis of a high temperature heat exchanger tube element.

Radiative heat transfer has been numerically studied since the 1960's. Because a gray analysis is much simpler than a non-gray one, a gray analysis has been adopted by many researchers. Echigo et al.<sup>(1)</sup> analyzed two-dimensional combined convective and radiative heat transfer with fully developed laminar flow of a gray gas in a pipe. They showed that the temperature profiles and the bulk mean temperatures obtained by the one-dimensional approximation

tended to be lower than those obtained by the two-dimensional evaluation of radiation for low values of the Graetz number. Schuler and Campo<sup>(2)</sup> numerically investigated combined convection and radiation of a turbulent gray flow for the thermally developing region of a circular pipe. The radiation contribution was modeled by the P-1 approximation. Huang and Lin<sup>(3)</sup> studied the interaction of gray radiation with laminar forced convection in thermally developing, circular pipe flow with a two-dimensional radiation model which included absorption, emission, and isotropic scattering. From their parametric study, they showed that the axial radiation effect becomes significant at small conduction-radiation ratios.

Unfortunately, it has been known that the gray analysis overestimated radiation heat transfer too much (see Seo et al.<sup>(4)</sup> and Hirano et al.<sup>(5)</sup>). Therefore, the non-gray assumption is more realistic and accurate than the gray one if the radiation properties of a medium strongly depend on the wave number.

Non-gray analyses have also been performed since the middle of the 1960's. DeSoto<sup>(6)</sup> considered the interaction of radiation with conduction and convection in a non-isothermal, non-gray gas ( $\text{CO}_2$ ) in a circular tube with isothermal black walls; the flow was hydrodynamically fully developed and thermally developing. The exponential wide band model<sup>(7)</sup> was used to represent the temperature and frequency dependence of the spectral absorption coefficients. He concluded that although the axial radiative component was large at the tube entrance, it decreased rather abruptly as the flow proceeded only a short distance ( $x^*=0.0042$ ) into the tube and, thereafter, its effect was very small. Wassel and Edwards<sup>(8)</sup> calculated the temperature profile and the convective and radiative heat fluxes for a fully developed laminar and turbulent flow of a non-gray gas in a cylinder.

They developed a table of Nusselt numbers for  $Re=16,900$ ,  $Re=80,650$ , and laminar flow. Because they considered a single band and evaluated dimensionless parameters from the single band, it is difficult to use their table for multiband gases and/or their mixtures.

Im and Ahluwalia<sup>(9)</sup> studied combined convective and radiative heat transfer in a rectangular duct with a non-gray gas. They considered simultaneously developing turbulent flow and heat transfer of a mixture of carbon dioxide, water vapor, and particles. They used the moment method, the exponential wide band parameters, and the Mie theory<sup>(10)</sup> to solve the radiation transfer equation. In addition, Ahluwalia and Im<sup>(11)</sup> considered the turbulent non-gray gas flow in a smooth tube using the same numerical approach as the method used in the work of Im and Ahluwalia<sup>(9)</sup>. Soufiani and Taine<sup>(12)</sup> considered non-gray radiation using a statistical narrow band model<sup>(13)</sup>. They applied this model to coupled radiation and convection in a laminar flow of the mixture of water vapor and the air between two parallel, isothermal walls but only showed the pure water vapor results. Hirano et al.<sup>(5)</sup> numerically analyzed heat transfer for fully developed laminar flow of a gray gas and a non-gray gas ( $\text{CO}_2$ ) between infinite parallel plates using a finite difference technique. The authors found that the conventional gray gas analysis overestimated the radiative heat flux and underestimated the convective heat flux. The differences between the gray and non-gray radiative heat fluxes were 15% at  $x^*=0.0014$  and 7% at  $x^*=0.0072$ , and the differences between the convective heat flux were 44% and 77%, respectively. In another paper, Hirano et al.<sup>(14)</sup> studied enhancement of radiative heat transfer by the use of a radiating plate between infinite parallel plates. A mixture of carbon dioxide, water vapor and nitrogen was used to simulate prod-

ucts of combustion. It was shown that by installing a solid plate in the gas flow, the heat transfer enhancement was 80% for carbon dioxide and 36% for combustion gas. Seo et al.<sup>(4)</sup> investigated combined convection and non-gray radiation in simultaneously developing laminar flow and heat transfer in a smooth tube using the exponential wide band model and the P-1 approximation. The mixture of carbon dioxide, water vapor, and nitrogen were used as the working gas. They found that both convective and radiative Nusselt numbers for simultaneously developing flow are greater than those for hydrodynamically fully developed and thermally developing flow. In addition, it was shown that a gray analysis could not predict the heat transfer characteristics of non-gray radiation.

From this literature review, it is found that information for combined convection and non-gray radiation in simultaneously developing turbulent flow and heat transfer is sparse. Because flows in heat exchanger tube elements are usually turbulent, information for turbulent flows is required to design heat exchangers more than that for laminar flows. Although combined convection and non-gray radiation in simultaneously developing turbulent flow and heat transfer was studied by several researchers, these turbulent results are not applicable to other problems which have different temperature, composition, and geometry conditions due to the characteristics of non-gray radiation. Therefore, usually an involved numerical analysis is required whenever we want to calculate combined convection and radiation in a smooth tube. In this study, combined convection and non-gray radiation in simultaneously developing turbulent flows and heat transfer is considered. The continuity, momentum, and energy equations are solved numerically using a finite difference technique. The bulk mean temperature, and the convective and radiative

Nusselt numbers are studied for various flow conditions, temperature differences and gas component combinations. The exponential wide band model parameters are used to obtain the spectral absorption coefficient of the gas mixture. Based on the results from the numerical model, a simple correlation to predict the radiative heat flux of non-gray turbulent flow in a smooth tube is suggested.

## 2. NUMERICAL MODELING

### 2.1 Governing equations

Combined convection and non-gray radiation of simultaneously developing turbulent flow and heat transfer is numerically investigated. In order to derive the governing equations, several assumptions are made :

- 1) The gas is incompressible and its physical properties are constant.
- 2) Axial diffusion and radiation of heat are negligible compared to radial diffusion and radiation.
- 3) Viscous energy dissipation is negligible.
- 4) The gas absorbs and emits radiation, but does not scatter.
- 5) The wall is black. Its temperature is constant and uniform.
- 6) The inlet temperature and velocity are uniform.

Based on these assumptions, the governing equations for a smooth tube are as follows :

$$\text{Continuity : } \frac{1}{r} \frac{\partial}{\partial r} (rv) + \frac{\partial u}{\partial x} = 0 \quad (1)$$

Momentum :

$$\begin{aligned} v \frac{\partial u}{\partial r} + u \frac{\partial u}{\partial x} = -\frac{1}{\rho} \frac{\partial P}{\partial x} \\ + \frac{1}{r} \frac{\partial}{\partial r} \left[ r(\nu_\epsilon + \nu_t) \frac{\partial u}{\partial r} \right] + \frac{\partial}{\partial r} \left[ r(\nu_\epsilon + \nu_t) \frac{\partial u}{\partial r} \right] \end{aligned} \quad (2)$$

$$v \frac{\partial u}{\partial r} + u \frac{\partial v}{\partial x} = -\frac{1}{\rho} \frac{\partial P}{\partial r} \quad (3)$$

$$+ \frac{\partial}{\partial r} \left[ \frac{1}{r} (\nu_t + \nu_t) \frac{\partial(\tau v)}{\partial r} \right] + \frac{\partial}{\partial x} \left[ (\nu_t + \nu_t) \frac{\partial v}{\partial x} \right]$$

Energy :

$$u \frac{\partial T}{\partial x} = \frac{1}{r} \frac{\partial}{\partial r} \left[ r \left( \frac{\nu_t}{Pr_t} + \frac{\nu_t}{Pr_t} \right) \frac{\partial T}{\partial r} \right] - \frac{1}{\rho c_p} \nabla \cdot \bar{q}_r \quad (4)$$

The velocities are time-averaged, and  $\nu_t$  and  $Pr_t$  are the eddy viscosity and turbulent Prandtl number, respectively. The turbulent Prandtl number is set as 0.9 and the turbulent eddy viscosity will be discussed in section 2.2.

Boundary conditions are :

$$\text{at } r=0 : \frac{\partial u}{\partial r} = \frac{\partial v}{\partial r} = \frac{\partial T}{\partial r} = 0 \quad (5)$$

$$\text{at } x=0 : u = u_{in}, T = T_{in} \quad (6)$$

In order to evaluate the radiative heat flux vector in Eq.(4), the P-1 approximation is used. The participating bands were divided into a number of subbands, and the absorption coefficient of each sub-band was assumed constant<sup>(17)</sup>. The radiation intensity for each sub-band is calculated using the following P-1 equation<sup>(18)</sup> :

$$\frac{1}{r} \frac{\partial}{\partial r} \left( \frac{r}{a_i} \frac{\partial G_i}{\partial r} \right) = 3a_i(G_i - 4e_{b_i}) \quad (7)$$

where

$$G_i = \int_{\lambda_i}^{\lambda_{i+1}} G_{\lambda} d\lambda \quad (8)$$

is the direction and band-integrated intensity. In addition, the exponential wide band model is used to obtain the spectral absorption coeffi-

cient.(see Seo et. al.<sup>(4)</sup>)

## 2.2 Turbulence Modeling

For closure of the governing equations, many turbulence models are available. The  $\kappa-\epsilon$  model, which is numerically stable and widely used, is selected to calculate turbulent quantities.

The eddy viscosity in the governing equations is presented in terms of the kinetic energy of turbulence and its dissipation rate<sup>(15)</sup>.

$$\nu_t = c_{\mu} \frac{k^2}{\epsilon} \quad (9)$$

The kinetic energy of turbulence and its dissipation rate are modeled by the following two equations<sup>(15)</sup> :

$$v \frac{\partial k}{\partial r} + u \frac{\partial k}{\partial x} = \frac{1}{r} \frac{\partial}{\partial r} \left( r \frac{\nu_t}{\sigma_k} \frac{\partial k}{\partial r} \right) + \frac{\partial}{\partial x} \left( \frac{\nu_t}{\sigma_k} \frac{\partial k}{\partial x} \right) + \nu_t \left( \frac{\partial u}{\partial r} \right)^2 - \epsilon \quad (10)$$

$$v \frac{\partial \epsilon}{\partial r} + u \frac{\partial \epsilon}{\partial x} = \frac{1}{r} \frac{\partial}{\partial r} \left( r \frac{\nu_t}{\sigma_{\epsilon}} \frac{\partial \epsilon}{\partial r} \right) + \frac{\partial}{\partial x} \left( \frac{\nu_t}{\sigma_{\epsilon}} \frac{\partial \epsilon}{\partial x} \right) + c_1 \frac{\epsilon}{k} \nu_t \left( \frac{\partial u}{\partial r} \right)^2 - c_2 \frac{\epsilon^2}{k} \quad (11)$$

where  $c_{\mu}=0.09$ ,  $c_1=1.44$ ,  $c_2=1.92$ ,  $\sigma_k=1.0$ ,  $\sigma_{\epsilon}=1.3$ .

The boundary condition for Eqs. (10) and (11) are as follows<sup>(15)</sup> :

$$\frac{k}{u\tau} = \frac{1}{\sqrt{c_{\mu}}} \quad (12)$$

$$\epsilon = \frac{u\tau^3}{0.41y} \quad (13)$$

Wall functions are used as boundary condi-

tions for the momentum and energy equations, because the turbulence model in this investigation is not generally applicable across the turbulent boundary layer<sup>(15), (16)</sup>. The wall functions are as follows :

$$u^+ = \frac{1}{0.41} \ln(y^+) + 5.0 \quad (14)$$

$$t^+ = 2.195 \ln y^+ + 13.2 Pr - 5.66 \quad (15)$$

In addition, the symmetry boundary conditions are given :

$$\frac{\partial k}{\partial r} = \frac{\partial \varepsilon}{\partial r} = 0 \text{ at } r=0 \quad (16)$$

In order to solve the governing equations, a commercially available computational fluid dynamics code, entitled PHOENICS, is used. PHOENICS uses a staggered grid formulation of the finite volume equation, similar to that outlined by Patankar<sup>(19)</sup>. The continuity, momentum, energy, turbulent kinetic energy, and dissipation equations are solved simultaneously. Uniform grids for the radial direction and non-uniform grid for the axial direction (20 × 137) are used and generated using Eq(17)

$$x = 0.1 \times 10^{-4} \times 1.05^{(j-1)} (\text{m}) \quad (17)$$

where  $x$  is the axial location of the center of the  $j^{\text{th}}$  control volume from the tube inlet.

To incorporate radiation into the calculations, a mixture of 12% carbon dioxide, 16% water vapor, and 72% nitrogen by volume was investigated to simulate the stoichiometric combustion products of propane. The diameter of the tube used for numerical investigation was 0.05m which is typical for the tube elements of high temperature wasted heat recovery systems. The inlet and wall temperatures are assumed to be

1,200K and 900K, respectively. In addition, four more different temperatures are used to study the effect of the inlet and wall temperatures on combined convection and non-gray radiation.

Total heat fluxes transferred from the wall are given as follows :

$$q_t = \frac{1}{R \cdot \Delta x} \left[ \int_0^R \rho u c_p T r dr \right]_{x+\Delta x} - \int_0^R \rho u c_p T r dr \Big|_x \quad (18)$$

Convective heat flux transferred from the wall are obtained from the wall function as follow :

$$q_c = \rho c_p \frac{(T_w - T_m) u_\tau}{t^+} \quad (19)$$

Therefore, radiative heat flux is the difference between total and convective heat flux.

$$q_r = q_t - q_c \quad (20)$$

From these heat fluxes, the total, convective, and radiative Nusselt numbers can be defined as :

$$Nu_t = \frac{q_t \cdot D}{k(T_w - T_m)} = Nu_c + Nu_r \quad (21)$$

$$Nu_c = \frac{q_c \cdot D}{k(T_w - T_m)} \quad (22)$$

$$Nu_r = \frac{q_r \cdot D}{k(T_w - T_m)} \quad (23)$$

### 3. EXPERIMENT

In order to verify the numerical modeling, experimental investigation has been carried out. For these experiments, a high temperature flow

loop has been built. As shown in Fig. 1, the flow loop consists of four major parts: the combustion system (the primary flow system), the secondary flow system, the test section, and the exhaust duct. The combustion system produces a high temperature gas flow by burning propane gas in air. The temperature range of the hot gas is from 570K to 1470K. A wide range of flowrates (0.005-0.09 kg/s) up to the maximum

design temperature can be obtained. Through the secondary flow line, relatively cold air is supplied to the test section. The variable power electric preheater was installed to control the secondary air temperature from ambient up to 770K. Using this preheater and the burners, many combinations of operating temperatures can be made in the test section.

The test section, which consisted of a shell and a tube, was built. A tube was made of a smooth Inconel tube ( $D=40.5\text{mm}$ ), and the shell of the test section was made of an Inconel pipe which was 1.22m long, 88.9mm OD, 82.6mm ID. Hot gas flow from the combustion chamber outlet and electrically heated air flow were directed into tubeside and shellside of the test section, respectively. The range of the bulk and wall temperature was from 540K to 1140K and from 400K to 730K. The experimental apparatus, the test section, the experimental method, etc. were described in Seo<sup>(20)</sup> in detail.

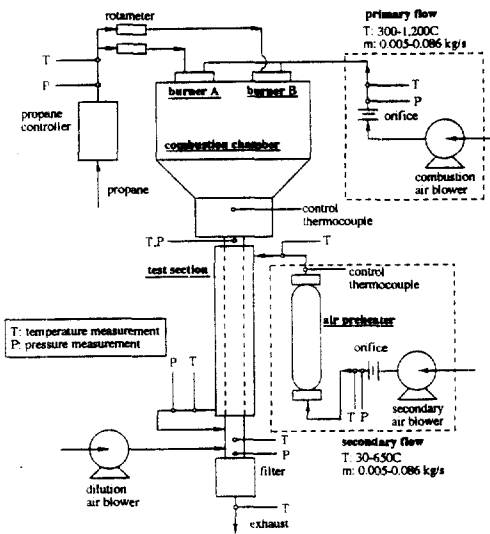


Fig.1 Schematic of the experimental apparatus

## 4. RESULTS

### 4.1 Verification

To validate the results of the model, pure con-

Table 1. Comparisons of pure convective Nusselt numbers for smooth tubes from various correlations ( $Re=15,000, Pr=0.807$ ) (Kakac<sup>22</sup>)

name	correlation	$Nu$	diff. (%)
Prandtl	$Nu = \frac{(f/2) Re Pr}{1 + 8.7(f/2)^{0.5}(Pr-1)}$	47.3	+8.9
McAdams	$Nu = 0.021 Re^{0.8} Pr^{0.4}$	42.9	-1.9
Petukov and Kirillov	$Nu = \frac{(f/2) Re Pr}{1.07 + 12.7(f/2)^{0.5}(Pr^{2/3} - 1)}$	43.9	+1.8
Webb	$Nu = \frac{(f/2) Re Pr}{1.07 + 9(f/2)^{0.5}(Pr-1)Pr^{-0.25}}$	44.3	+2.7
Keys and Crawford	$Nu = 0.022 Re^{0.8} Pr^{0.5}$	43.3	+0.5
the present work		43.1	

where  $\text{diff.}(\%) = (Nu_{\text{correlation}} - Nu_{\text{present}}) / Nu_{\text{present}}$

vective Nusselt numbers without radiation are compared in Tabel 1 to the well-known correlations for fully developed Nusselt number in a smooth tube. As shown in the table, the calculated convective Nusselt number is reasonably close to the Nusselt numbers from these correlations except for Prandtl's correlation. (The differences between the calculated Nusselt number and the correlations are much smaller than the suggested uncertainty (about 5~6%) of the correlations.)

In addition, the numerical method was verified by comparison with experimental data of Seo<sup>(20)</sup> and Edwards et al<sup>(21)</sup>. In Fig. 2 a comparison of the experimental and numerical results are shown. It is found from this figure that the present numerical model can accurately predict combined convection and non-gray radiation for a wide range of a Reynolds number (6,000~55,000) and ratio of wall-to-bulk temperature ( $T_w/T_b$ ) (0.6~0.7). Although there are a few other experimental studies for high temperature heat transfer reported in the literature, it is impossible to compare those results to the present numerical results, because each experimental study differs in geometry, temperature conditions, and gas compositions. Non-gray radiation heat transfer is a nonlinear function of temperature, partial pressure of participating media, and geometry. Hence, results which have been published for certain conditions cannot be applied to other situations unless every condition is identical.

#### 4.2 Results and discussion

For convection with and without radiation in a smooth tube, the bulk mean temperature and Nusselt number variations are shown in Figs. 3 and 4, respectively. In Fig.3, in order to show the effect of the average temperature ( $(T_{in} + T_w)/2$ ) and the temperature difference ( $T_{in} - T_w$ ) on radiation heat transfer in a smooth tube, five

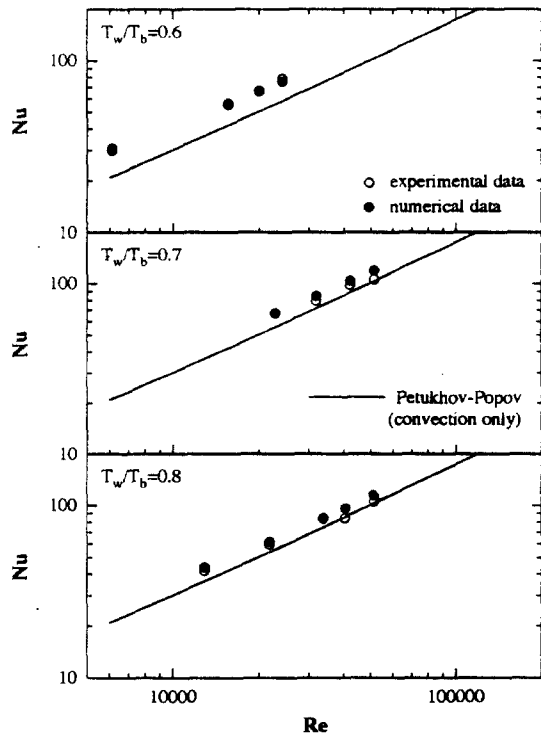


Fig.2 Comparison of the experimental and numerical length-averaged Nusselt numbers for smooth tubes Petukhov-Popov (Kakac, 1987) :

$$Nu = \frac{(C_f/2) Re Pr}{(1 + 13.6C_f) + (11.7 - 1.8Pr^{-1/3})(C_f/2)^{1/2}(Pr^{2/3} - 1)}$$

different temperature pairs are used : A)  $T_{in} = 1,200K$  and  $T_w = 900K$ ; B)  $T_{in} = 1,200K$  and  $T_w = 600K$ ; C)  $T_{in} = 900K$  and  $T_w = 600K$ ; D)  $T_{in} = 900K$  and  $T_w = 300K$ ; E)  $T_{in} = 600K$  and  $T_w = 300K$ . All of the bulk mean temperatures for the five different temperature pairs with combined convection and radiation decrease faster than those for pure convection. (These are about 5~9% lower than those for pure convection at  $x^* = 0.0027$ . Refer to Table 2.) However, the differences between the bulk mean temperatures for the five temperature pairs and the bulk mean temperature for pure convection are much smaller than that for laminar flow in a



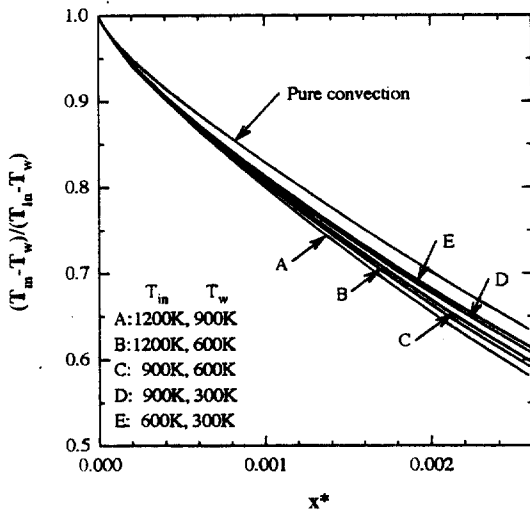


Fig.3 The bulk mean temperature variation for the five different inlet and wall temperatures  
 ( $Re=15,000, D=0.05, Y_{CO_2}=0.12, Y_{H_2O}=0.16, Y_{N_2}=0.72$ )

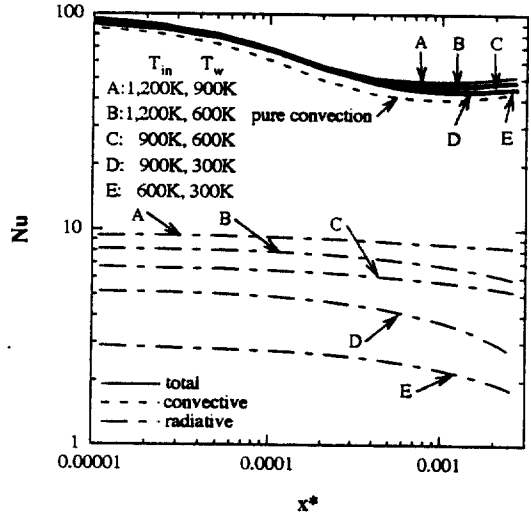


Fig.4 The total, convective, and radiative Nusselt number variation for the five different inlet and wall temperatures  
 ( $Re=15,000, D=0.05m, Y_{CO_2}=0.12, Y_{H_2O}=0.16, Y_{N_2}=0.72$ )

Table 2. Comparisons of calculated data for different temperature conditions  
 ( $x=1.6m, Y_{CO_2}=0.12, Y_{H_2O}=0.16, D=0.05m, Re=15,000$ )

Temperature ( $T_{in}, T_w$ )	$\theta_m$	diff.(%)	$Nu_t$	diff.(%)
1,200K, 900K	0.581	-8.5	51.27	18.8
1,200K, 600K	0.589	-7.3	48.82	13.2
900K, 600K	0.592	-6.8	47.92	11.1
900K, 300K	0.601	-5.3	45.41	5.3
600K, 300K	0.607	-4.5	44.45	3.0
pure convection	0.635		43.14	

where  $diff.(%) = (\theta_m - \theta_{m,conv})/\theta_{m,conv}$  or  $(Nu_t - Nu_c)/Nu_c$

smooth tube(refer to Seo et al., (4)). As could be expected, we can conclude that the role of radiation heat transfer in turbulent flow becomes relatively smaller than that in a laminar flow, and turbulent convection becomes dominant. Note that the difference between the inlet and wall temperatures is not as important to radiation as the average temperature.

The total, convective, and radiative Nusselt numbers are shown in Fig.4, and the total Nusselt number difference between pure convection and combined convection and radiation is presented in Table 2. From the table, it is seen that radiation heat transfer is important at high temperatures although turbulent convection is significant. In Fig.4, the convective Nusselt

numbers for the five cases are not presented, because those are very close to the pure convection Nusselt number and it is difficult to see the differences. Although the radiative Nusselt numbers are very different from each other, the total Nusselt numbers do not differ much because convective heat transfer is relatively strong in turbulent flow. Of the five cases studied, the radiative Nusselt number for  $T_{in}=1,200\text{K}$  and  $T_w=900\text{K}$  is the largest and is only about 16% of the total Nusselt number. The radiative heat transfer role decreases as the average temperature decreases. The radiative Nusselt number for  $T_{in}=600\text{K}$  and  $T_w=300\text{K}$  is less than 4% of the total Nusselt number. Thus, radiation heat transfer could be neglected for this condition ( $Y_{CO_2}=0.12$ ,  $Y_{H_2O}=0.16$ ,  $D=0.05\text{m}$ ,

$Re=15,000$ ,  $T_{in}=600\text{K}$ , and  $T_w=300\text{K}$ ) without a significant loss in accuracy. However, if the mole fractions of the participating media increased significantly and/or the tube diameter increased, radiation heat transfer would be important with even low temperatures and should not be ignored. The radiative Nusselt numbers vary little over a wide range of  $x^*$ , while the convective Nusselt number decreases dramatically near the inlet of the tube. The differences between the total Nusselt numbers appear far downstream ( $x^*>0.0003$ ) where radiation heat transfer becomes more important.

In Figs. 5a and b, the bulk mean temperature variation and the Nusselt number for different gas mixtures are plotted. Mixture A ( $Y_{CO_2}=0.12$ ,  $Y_{H_2O}=0.16$ ,  $Y_{N_2}=0.72$ ,  $Y_{O_2}=0.0$ ) is the stoi-

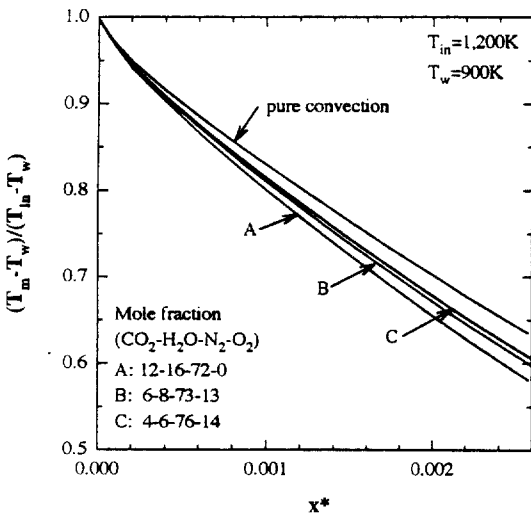


Fig.5a The bulk mean temperature variation for the different gas composition. Mixture A represents the stoichiometric combustion products of propane. Mixture B and C represent the stoichiometric combustion products of propane with 100% and 200% excess air respectively. ( $Re=15,000$ ,  $D=0.05\text{m}$ ,  $Y_{CO_2}=0.12$ ,  $Y_{H_2O}=0.16$ ,  $Y_{N_2}=0.72$ )

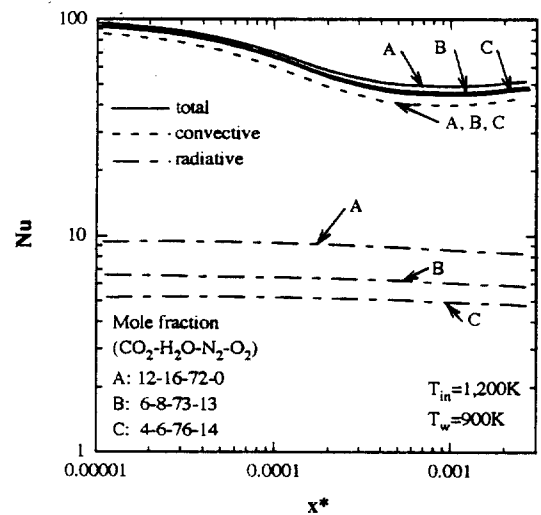
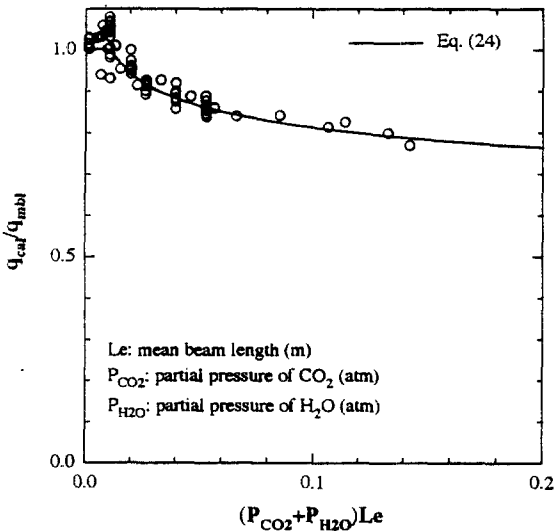


Fig.5b The total, convective, and radiative Nusselt number variation for the different gas composition. Mixture A represents the stoichiometric combustion products of propane. Mixture B and C represent the stoichiometric combustion products of propane with 100% and 200% excess air, respectively. ( $Re=15,000$ ,  $D=0.05\text{m}$ ,  $Y_{CO_2}=0.12$ ,  $Y_{H_2O}=0.16$ ,  $Y_{N_2}=0.72$ )

chiometric combustion products of propane and mixtures B ( $Y_{CO_2}=0.06$ ,  $Y_{H_2O}=0.08$ ,  $Y_{N_2}=0.73$ ,  $Y_{O_2}=0.13$ ) and C ( $Y_{CO_2}=0.04$ ,  $Y_{H_2O}=0.06$ ,  $Y_{N_2}=0.76$ ,  $Y_{O_2}=0.14$ ) represent theoretical combustion products of propane with 100% and 200% excess air, respectively. The bulk mean temperature variation between different mixtures is not significant. In addition, the total Nusselt numbers are very close to each other even though the radiative Nusselt numbers are very different, again demonstrating that turbulent convection is dominant. However, the radiative Nusselt numbers are still more than about 10% of the total Nusselt number at  $x^*=0.0027$ , even though 100% and 200% excess air is used.

## 5. CORRELATION

A simple and convenient method is needed to



**Fig.6** The ratio of radiative heat flux calculated by the present simulation to the radiative heat flux evaluated by the mean beam length model in smooth tubes. ( $D=0.05-0.5$  m,  $T_{in}=600-1200$  K,  $\Delta T(=T_{in}-T_w)=200-600$  K,  $P_{CO_2}=0.01-0.20$  atm,  $P_{H_2O}=0.01-0.02$  atm,  $P_t=1$  atm)

calculate the radiation contribution when convection and radiation are present in an intube turbulent flow. The radiation contribution then could be used with Eq. (21) and the pure convection Nusselt number to calculate either the total Nusselt number or heat flux. Hence, the axially local radiation heat flux ( $q_{cal}$ ) calculated by the present numerical simulation and the radiation heat flux ( $q_{mbl}$ ) evaluated by the mean beam length model<sup>(10)</sup> are compared on Fig.6. In this figure, the ratio  $q_{cal}/q_{mbl}$  is presented with respect to  $(P_{CO_2}+P_{H_2O})Le$ . (In this figure, data points are scattered. The logarithmic-scaled graph for total emittances of both carbon dioxide and water vapor was small so that reading error might be large for some conditions.) For the comparisons, combinations of conditions over a wide range of operating conditions were used;  $D=0.05-0.5$  m,  $T_{in}=600-1200$  K,  $\Delta T(=T_{in}-T_w)=200-600$  K,  $Re=10,000-50,000$ ,  $P_{CO_2}=0.01-0.20$  atm,  $P_{H_2O}=0.01-0.20$  atm,  $P_t=1$  atm. As can be seen, the non-gray radiative heat flux does correlate simply with the mean beam length model. Using this figure, the relationship between  $q_{cal}$  and  $q_{mbl}$  can be formulated as follow :

$$q_{cal} = q_{mbl} \cdot F_t \quad (24)$$

$$\text{where } F_t = [100(P_{CO_2} + P_{H_2O})Le]^{-0.09}$$

$$\text{for } (P_{CO_2} + P_{H_2O})Le \geq 0.01$$

$$\text{or } F_t = 1.0 \text{ for } (P_{CO_2} + P_{H_2O})Le < 0.01$$

Using this relationship, the non-gray radiation Nusselt number in a smooth tube with turbulent flow can be predicted to within  $\pm 10\%$  using the radiative heat flux obtained by the mean beam length model. For this calculation, the bulk mean temperature is used as the gas temperature.  $q_{cal}$  calculated by Eq. (24) is the

axially local radiation heat flux for the region  $x^* > 0.0005$ , and this correlation (Eq.(24)) is not applicable to radiation heat flux calculation near the inlet. The downstream temperature profile is different from that near the inlet, and the temperature profile near the inlet is very flat. This means that radiation heat flux near the inlet can be approximated by the mean beam length model without the correction factor ( $F_c$ ). In other words,  $q_{rad}/q_{mbl}$  is close to unity near the inlet.

In order to evaluate the performance of heat exchangers, the length-averaged Nusselt number is preferred to the local value. Fortunately, as was shown in the Fig.4, the radiative Nusselt number varies little compared to the convective Nusselt number so that the difference between the local and the length-averaged value is small. Although this difference increases as radiation becomes weak compared to convection, it is not a significant problem, because the effect on the total Nusselt number (which is the sum of the convective and radiative Nusselt numbers) is still small. From sample calculations, it is found that although the local radiative Nusselt number is used to calculate the length-averaged total Nusselt number, the difference is usually less than 2% and the maximum difference is not greater than 5%.

## 6. CONCLUSIONS

Combined convection and non-gray radiation with simultaneously developing turbulent flow and heat transfer in a smooth tube has been numerically investigated using a finite difference technique. Based on results obtained, several conclusions can be drawn.

Radiation heat transfer becomes significant when average temperature  $((T_{in} + T_w)/2)$  is high and the temperature difference  $(T_{in} - T_w)$  is large. However, the role of radiation heat trans-

fer is relatively small in turbulent flow compared to that for laminar flow for the present operating condition ( $T_{in} = 600 - 1,200\text{K}$ ,  $T_w = 300 - 900\text{K}$ ,  $Re = 15,000$ ,  $D = 0.05\text{m}$ ,  $Y_{CO_2} = 0.12$ ,  $Y_{H_2O} = 0.16$ ,  $Y_{N_2} = 0.72$ ). Radiation heat transfer becomes important as the average temperature, mole fractions of participating gases, and the diameter of the tube increase. As found in the laminar flow investigation, convective Nusselt numbers are almost independent of radiation heat transfer, and radiative Nusselt numbers vary little over a wide range of  $x^*$ . A simple correlation to predict the radiative heat flux in a smooth tube is suggested (see Eq. (24)) using the mean beam length model. From this correlation, the radiative heat flux in turbulent flow in a smooth tube can be predicted with 10% error, and the total Nusselt number could be obtained within 5% error with well-known correlations for fully developed convection Nusselt number in smooth tubes.

## REFERENCES

1. Echigo, R., Hasegawa, S., and Kamiuto, K., 1975, "Composite Heat Transfer in a Pipe with Thermal Radiation of Two Dimensional Propagation-in Connection with the Temperature Rise in Flowing Medium Upstream from Heating Section", International Journal of Heat and Mass Transfer, Vol. 18, pp. 1149~1159.
2. Schuler, C., and Campo, 1988, "Numerical Prediction of Turbulent Heat Transfer in Gas Pipe Flows Subject to Combined Convection and Radiation", International Journal of Heat and Fluid Flow, Vol. 99, pp. 308~315.
3. Huang, J. M., and Lin, J. D., 1991, "Combined Radiative and Forced Convective Heat Transfer in Thermally-Developing Laminar Flow Through a Circular Pipe",

- Chemical Engineer Communication, Vol. 101, pp. 147~164.
4. Seo, T., Kaminski, D. A., and Jensen, M. K., 1994, "Combined Convection and Radiation in simultaneously Developing Flow and Heat Transfer with Non-gray Gas Mixtures", Numerical Heat Transfer, Part A, 26, pp. 49~66.
  5. Hirano, M., Miyauchi, T., and Takahira, Y., 1988 "Heat Transfer Analysis of a Nongray Gas in a Flow System(Part 1. The Case of Small Temperature Differences between the Gas and a Heat Absorbing Surface)", Heat Transfer-Japanese Research, Vol. 17, no. 2, pp. 65~79.
  6. Desoto, S., 1968, "Coupled Radiation, Conduction and Convection in Entrance Region Flow", International Journal of Heat and Mass transfer, Vol. 11, pp. 39~53.
  7. Edwards, D. K., 1976, "Molecular Gas Band Radiation", Advances in Heat Transfer, Vol. 12, pp. 115~193, Academic Press, New York.
  8. Wassel, A. T., and Edwards, D. K., 1976, "Molecular Gas Radiation in a Laminar or Turbulent Pipe Flow", ASME Journal of Heat Transfer, Vol. 98, pp. 101~107.
  9. Im, K. H., and Ahluwalia, R. K., 1984, "Combined Convective and Radiation in Rectangular Ducts", International Journal of Heat and Mass Transfer, Vol. 27, pp. 221~231.
  10. Siegel, R., and Howell, J. R., 1981, Thermal Radiation Heat Transfer, 2nd ed., Hemisphere Publishing Co., New York.
  11. Ahluwalia, R. K., and Im, K. H., 1984, "Radiation Heat Transfer in Segregated Media", AIAA JOURNAL, Vol. 22, No. 2, pp. 317~319.
  12. Soufiani, A., and Taine, J., 1987, "Application of Statistical Narrow Band Model to Coupled Radiation and Convection at High Temperature", International Journal of Heat and Mass Transfer, Vol. 30, No. 3, pp. 437~447.
  13. Soufiani, A., Hartmann, J. M., and Taine, J., 1985, "Validity of Band Model Calculations for  $\text{CO}_2$  and  $\text{H}_2\text{O}$  Applied to Radiative Properties and Conductive Radiative Transfer", Journal of Quantitative Spectroscopic and Radiative Transfer, Vol. 33, pp. 243~257.
  14. Hirano, M., Miyauchi, T., and Takahira, Y., 1988, "Enhancement of Radiative Heat Transfer in the Laminar Channel Flow of Non-gray Gases", International Journal of Heat and Mass Transfer, Vol. 31, pp. 367~374.
  15. Rodi, W., 1980, Turbulence models and Their Application in Hydraulics, a State of the Art Review, Publication of International Association for Hydraulic Research, Delft, Netherlands.
  16. Kays, W. M. and Crawford, M. E., 1980, Convective Heat and Mass Transfer, 2nd Ed., McGraw-Hill Book Co., New York.
  17. Kaminski, D. A., and Moder, J. P., 1989, "A Nongray P-n Approximation for Radiative Transfer", National Heat Transfer Conference, HTD-Vol. 106, pp. 27~34.
  18. Ozisik, M. N., 1973, Radiation Transfer and Interactions with conduction and Convection, Wiley, New York.
  19. Patankar, S. V., 1980, Numerical Heat Transfer and Fluid Flow, McGraw-Hill, NY.
  20. Seo, T., 1994, "Combined Convection and Non-Gray Radiation in Simultaneously developing flow and heat transfer", Ph. D. dissertation, Rensselaer Polytechnic Institute, Troy, NY.
  21. Edwards, D. P., Seo, T., Jensen, M. K., and Kaminski, D. A., 1995, "An Investigation of Heat Transfer in Longitudinally Finned Ce-

- ramic Tubes”, 4th ASME/JSME Thermal Engineering Joint Conference, Hawaii, March.
22. Kakac, S., 1987, “The Effect of Temperature Dependent Fluid Properties on Convective Heat Transfer”, Handbook of Single Phase Convective Heat Transfer, S. Kakac, R. K. Shah, and W. Aung, eds., J. Wiley and Sons, New York.